

VIRGO	N T S 9 6 0 3 8
Henrich Heitmann 18.06.1996	Measurement of position and orientation of the input mode cleaner masses

A system is described allowing to measure the position and orientation of the suspended MC masses from outside the vacuum chamber. The necessary optical setup consists of a CCD camera (Annecy camera), two lasers whose beams are reflected on a mirror fixed on the mass, an auxiliary mirror and two or four colour marks on the mass. The system generates light spots on the CCD; the formulae necessary for deducing the mass position from the spot positions are described, as well as the results of noise and long term stability measurements. It is shown that a single camera is sufficient for measuring six degrees of freedom. The achievable short-term rms error integrated over 1/60 sec is equal to or better than 1 $\mu\text{m}/\mu\text{rad}$ for translation and rotation, except θ_z (20 μm).

As opposed to global mass control, where the reference values come from a global quantity like cavity length or relative alignment of different mirrors with respect to each other, the local control compares the mass position with respect to ground (local reference

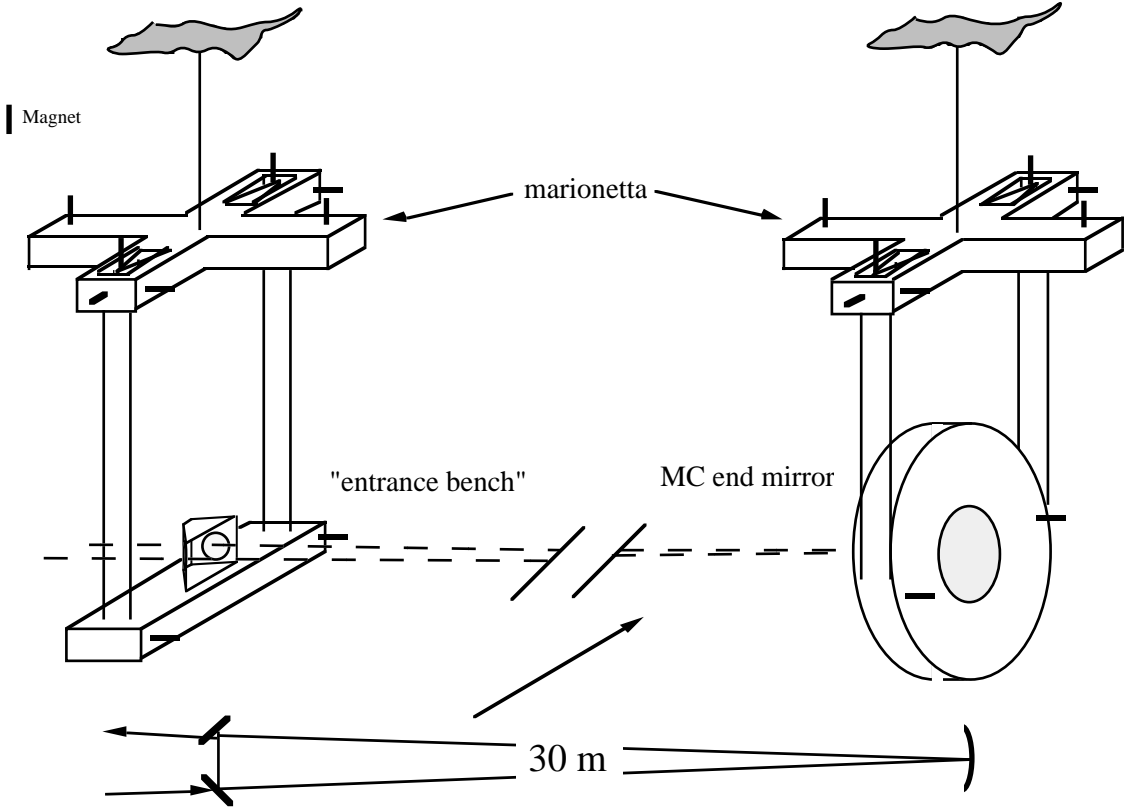


Fig. 1: Orsay 30m mode cleaner prototype; mass 1, with two flat mirrors, is left; mass two, with the curved mirror, right. The 144m VIRGO mode cleaner has 3 seismic filter stages above the marionetta. The schematic path of the VIRGO laser beam in the MC is shown below, seen from above.

system). There is a threefold need for determining locally the position of the suspended masses of the mode cleaner:

- *storing the position in memory*: The mass position is continuously monitored (or stored once after the first alignment is finished) and, in case of a fault (out-of-lock condition...), the last position can be read from memory and restored manually or by computer, thus avoiding a completely new alignment starting from zero.
- *compensating slow angular drifts*: During the prealignment phase, the mass positions must be kept stable enough such that one mass does not move while the other one is being aligned.
- *damping of the pendular motions*: The pendulum Q should be reduced to quite close to unity in order to avoid excessive mass movements excited by forces acting on the mass during the prealignment. During VIRGO operation, no local damping should be necessary, since the masses are controlled by global control loops.

Use of a CCD camera (Annecy camera system [4]) for local position measurement was proposed in [2]; there, the use of three cameras per mass was suggested. Here it will be shown, that one camera is sufficient for measuring all six degrees of freedom with good precision.

Two different schemes are presented: a coarse one, having low resolution, but a large dynamic range for prealignment of the masses when they are far from their final alignment; and a fine one, for high precision measurements when the masses are already approximately well positioned.

Fine measurement scheme

The optical scheme uses two color marks on the mass, and a direct and a folded laser beam with an auxiliary mirror (Fig. 2). The mass is supposed to have a reflecting (mirror) surface, otherwise an auxiliary mirror must be fixed to it. With this scheme, the camera image consists of 4 bright spots; the positions of these spots yield the information necessary to determine the 3 translational and the 3 rotational degrees of freedom of the observed mass.

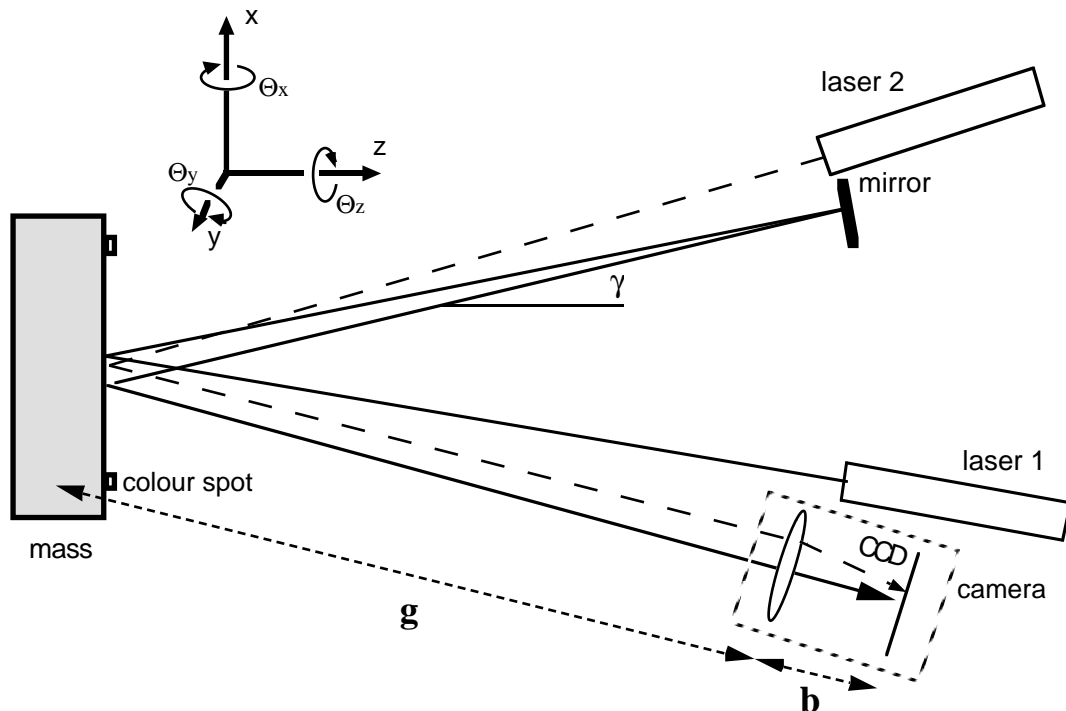


Fig. 2: Fine scheme for determining mass position/orientation, seen from above (against the y direction). Laser 1 (folded beam) serves for determining θ_x, θ_y ; the image of the two points on the CCD gives x, y and θ_z ; laser 2 (direct beam) gives informations on z . $1/f = 1/b + 1/g$.

At the same time, laser beams and features on the mass are observed. One might think that this requires the use of two cameras, one without lens and one with. However, this is not the case. The use of the lens also for looking at the laser beams has even the advantage of better decoupling the measurements of the degrees of freedom (see Appendix 2). Thus, the direct beam carries only information about the z direction (independently of θ_x and θ_y). On the other hand, the folded beam, because of its double trajectory, is only sensitive to θ_x and θ_y , and not to z. x and y are measured by looking at the displacement of the reference marks, and θ_z by their rotation.

For determining the mass position, a reference position must be defined; the camera software determines the *deviations* x,y,z and $\theta_x,\theta_y,\theta_z$ from the reference position. The corresponding *deviations* of the spot positions on the sensitive surface of the camera are denoted by x_i,y_i , where i is 1 / 2 for the left / right color mark, and 3 / 4 for the direct / folded beam.¹ $d = b+g$ is the camera-mass distance, D_x the distance of the two color marks on the mass. If d and the lens focal length f are known, g, b and the magnification A can be calculated:

$$g = \frac{d}{2}(1+q), \quad b = \frac{d}{2}(1-q), \quad A = \frac{b}{g} = \frac{1-q}{1+q} \quad \text{with} \quad q = \sqrt{1 - \frac{4f}{d}} \quad .$$

Assumptions: The reference position is more or less aligned with the x,y and z axes; the deviations of the actual position from the reference position are small, and rotations are around the center of the reflecting surface. The color marks are placed on a horizontal line symmetric to the origin (center of rotation) of the mass. The lens is focused such as to give a sharp image of the mass surface.

Formulae (fine)

Two configurations are considered: camera with and without lens. Without lens, not all position informations can be obtained, since only the laser beams can be observed.

Spot displacements on the camera

With lens

$$x_{1/2} = - \frac{A}{1 \mp n_x \sin \gamma} \frac{x \cos \gamma + (z \mp \frac{D_x}{2} \theta_y) (\sin \gamma \mp n_x)}{1 \mp n_x \sin \gamma}$$

$$y_{1/2} = - \frac{A}{1 \mp n_x \sin \gamma} (y \pm \frac{D_x}{2} \theta_z)$$

Without lens

$$x_3 = -2d \theta_y + 2z \tan \gamma$$

$$y_3 = 2d \theta_x \cos \gamma$$

$$x_4 = -8d \theta_y$$

$$y_4 = 8d \theta_x \cos \gamma$$

With lens

$$x_3 = -A 2z \sin \gamma$$

$$y_3 = 0$$

$$x_4 = A 4g \theta_y$$

$$y_4 = -A 4g \theta_x \cos \gamma$$

Mass position changes

Without lens

With lens

¹The local camera coordinate system is turned with respect to the mass coordinate system by the angle γ , in order to have the sensitive surface in the x-y plane.

$$\begin{aligned}
x & \text{ ---} \\
y & \text{ ---} \\
z & = \frac{x_3 + 2d\theta_y}{2 \tan \gamma} \\
\theta_x & = \frac{y_4}{8d \cos \gamma} \\
\theta_y & = -\frac{x_4}{8d} \\
\theta_z & \text{ ---} \\
x^* & = -z \tan \gamma - \frac{x_1 + x_2}{2A \cos \gamma} \\
y & = -\frac{(y_1 + y_2) + (y_2 - y_1) n_x \sin \gamma}{2A} \\
z & = -\frac{x_3}{2A \sin \gamma} \\
\theta_x & = -\frac{y_4}{4gA \cos \gamma} \\
\theta_y & = \frac{x_4}{4gA} \\
\theta_z & = -\frac{(y_1 - y_2) - (y_1 + y_2) n_x \sin \gamma}{AD_x} \\
& \quad \left(n_x = \frac{D_x}{2g}, \text{ angles in rad} \right)
\end{aligned}$$

The sensitivity for z , θ_x and θ_y measurements is bigger by about a factor A without the lens. However, experience shows that the sensitivity of the laser beams is very high anyway, such that one rather has the interest to increase the dynamic range of the measurement by using a lens, rather than to further increase the sensitivity by using the camera without lens.

If the optical scheme is different from Fig. 2 (e.g. camera is on the other side), then the signs in the formulae must be changed accordingly.

Coarse measurement scheme

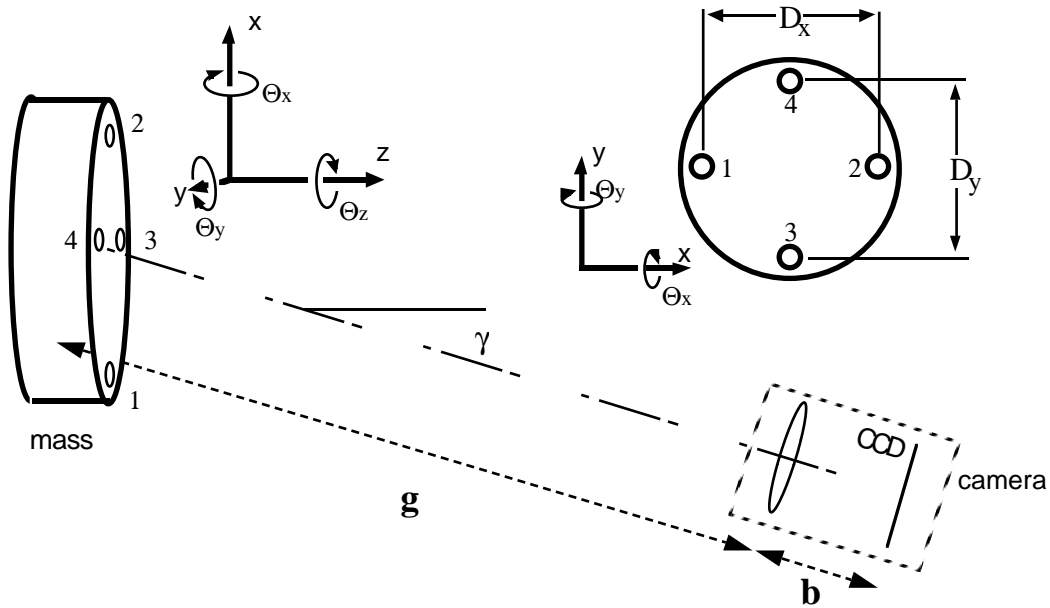


Fig. 3: Coarse scheme for determining the mass position without lasers, seen from above (against the y direction).

During the phase of initial alignment it may happen that the mass is strongly misaligned, such that the laser beams will not hit the CCD at all. In this case, one can determine the 6 degrees of freedom of the mass by observing 4 color marks on the mass, although the

*Approximation for $n_x \ll 1$. The full formula is

$$x = -z \tan \gamma - \frac{(x_1 + x_2) (1 + n_x^2 \sin^2 \gamma) + (x_2 - x_1) 2n_x \sin \gamma + \theta_y AD_x n_x}{2A \cos \gamma}$$

precision is less (Fig. 3). Since one wants to switch between the two modes of measurement according to the state of alignment and the desired precision, the optical configuration here must be the same as for the previous scheme; the lasers are not used, hence not drawn.

The deviations of the spot positions on the camera surface are denoted by x_i, y_i , where i is 1 / 2 / 3 / 4 for the left / right / lower / upper color mark. $D_{x/y}$ the distance between the horizontal/vertical color marks on the mass. Again it is assumed, that the deviations of the actual position from the reference position are small, that the lens is focused such as to give a sharp image of the mass surface, and that rotations are around the center of the reflecting surface.

Formulae (coarse)

Spot displacements on the camera

$$x_{1/2} = - \frac{A}{1 \mp n_x \sin \gamma} \frac{x \cos \gamma + (z \mp \frac{D_x}{2} \theta_y) (\sin \gamma \mp n_x)}{1 \mp n_x \sin \gamma}$$

$$y_{1/2} = - \frac{A}{1 \mp n_x \sin \gamma} (y \pm \frac{D_x}{2} \theta_z)$$

$$x_{3/4} = - A \left[(x \mp \frac{D_y}{2} \theta_z) \cos \gamma + (z \pm \frac{D_y}{2} \theta_x) \sin \gamma \right]$$

$$y_{3/4} = - A \left[y - n_y \left((\frac{D_y}{2} \theta_x \pm z) \cos \gamma + (\frac{D_y}{2} \theta_z \mp x) \sin \gamma \right) \right]$$

Mass position changes

$$x = - \frac{\frac{D_y}{2} (x_3 + x_4) \cos \gamma - (y_4 - y_3) g \sin \gamma}{A D_y}$$

$$y = - \frac{(y_1 + y_2) + (y_2 - y_1) n_x \sin \gamma}{2A}$$

$$z = - \frac{\frac{D_y}{2} (x_3 + x_4) \sin \gamma + (y_4 - y_3) g \cos \gamma}{A D_y}$$

$$\theta_x = - \frac{x_3 - x_4}{A D_y \sin \gamma} + \frac{\theta_z}{\tan \gamma}$$

$$\theta_y^* = - \frac{(x_2 - x_1) + (x_1 + x_2) n_x \sin \gamma - (y_4 - y_3) \cos \gamma \frac{n_x}{n_y}}{A D_x \sin \gamma}$$

* Valid for $n_x \ll 1$. The full formula is

$$\theta_y = - \frac{((x_2 - x_1) + (x_1 + x_2) n_x \sin \gamma) (1 + n_x^2 (\cos^2 \gamma - 1)) - (y_4 - y_3) \cos \gamma \frac{n_x}{n_y}}{A D_x \sin \gamma (1 - n_x^2)}$$

$$\theta_z = - \frac{(y_1 - y_2) - (y_1 + y_2) n_x \sin \gamma}{AD_x} \quad (n_{x/y} = \frac{D_{x/y}}{2g}, \text{ angles in rad})$$

The perspective change in the distance between the images of mark 3 and 4 is used to measure z , which leads to a small precision for this variable. Due to the observation angle γ , the measurements in x and z are coupled, such that also the x precision suffers (see Tab. 1).

In all fine and coarse formulae, an inverted image due the lens is supposed. If also camera software etc. introduce an inversion, then care must be taken to respect the changed signs of x_i and/or y_i . The numbering of x_i, y_i is with respect to the mass (Fig. 3), not the image.

Comparison of both schemes

According to [2], the theoretical and experimental measurement accuracy of the Annecy camera system, as limited by the camera pixel noise, is 50 nm for determining the center position of a light spot at the frame rate of 60 Hz. This value was verified with the statistical procedure described below; a light spot was generated on the CCD surface by a halogen lamp and a metal plate with a 0.5 mm hole rigidly fixed to the camera. Taking into account the 1/60 sec integration time, the measured rms value of 50 nm corresponds to a spot position noise of $10^{-8} \text{ m}/\sqrt{\text{Hz}}$. From this, one can calculate the theoretical resolution for the mass positions, using the following values: spot distances on the mass: $D_x = D_y = 20 \text{ mm}$, camera lens $\varnothing = 50 \text{ mm}$, focal length $f = 150 \text{ mm}$, distance camera/mass $d = 1 \text{ m}$, angle $\gamma = 30^\circ$, magnification $A = 0.22$. For calculating the dynamic range, an allowed spot displacement on the CCD of 2 mm was supposed.

	half dynam. range			rms noise (60 Hz)		
	coarse	fine		coarse	fine	
x	10	10	mm	6	0.2	μm
y	9	9	"	0.15	0.15	"
z	18	9	"	11	0.2	"
θ_x	40°	3 mrad		40	0.08	μrad
θ_y	40°	3 mrad		30	0.07	"
θ_z	25°	25°		15	15	"

Tab. 1: Comparison of the theoretical performances of the two measurement schemes

Experimental results

A table top experiment was mounted [3,4] to test the fine scheme presented above. A $\varnothing = 25 \text{ mm}$ mirror with two white colour spots simulated the mode cleaner mass; its mounting permitted to vary the parameters x, y, z, θ_x and θ_y . The mass was illuminated by a Tungsten halogen lamp with integrated reflector, in order to achieve a sufficient brightness of the reference mark images. Laser 1 was a focusable 2 mW visible semiconductor laser, laser 2 a 0.5 mW HeNe laser, both with attenuators for avoiding camera saturation. The camera was a Reticon MC9000 series CCD with a 10x10mm (256x256 pixels à 40 μm) sensitive surface and a frame rate of 60 Hz [2]. The camera was read out by computer (VME + workstation), and the position calculations were carried out according to the above formulae by the camera software GalaXie [1]. Linearity, scale factors etc. were verified; the results corresponded to expectations [4].

The mass parameters were calculated by GalaXie at a rate of about 10 Hz; the values were regularly transmitted to a separate program performing statistical calculations. Every 400 sec, for 25 subsequent mass position samples the average and standard deviation was calculated. These measurements were performed over several days; the results are shown in Fig. 5. The evolution of the average shows the long term drifts of

the measurement error; the result of the standard deviation measurements corresponds to the rms fluctuations of the apparent mass position, averaged over the integration time of one frame (1/60 sec); its time behaviour is shown in Fig. 5b for each degree of freedom. Moreover, the evolution of the air temperature is plotted for comparison with the measurement error. After four days, the whole experiment was covered with a 1x2x0.5 m Plexiglas box in order to reduce the influence of air currents, dust and the like. The result, as can be seen in the figure, is quite remarkable: the apparent rms mass fluctuations are reduced by a factor of 3 to 10; the long term drift is not influenced, but the curve is smoother due to the reduced fluctuations. The mass position jumps at $t=4.5$ d are probably due to a misalignment during the box installation.

Fig. 6 shows the result of another measurement. Here the setup was protected by the box all the time; moreover, the temperature of the optical table and the air temperature were monitored in order to see correlations with daily fluctuations of the measured values. For the y degree of freedom, the thermal expansion of the 20 cm long rod carrying the mirror, calculated for an aluminium expansion coefficient of $2.4 \cdot 10^{-5}/^{\circ}\text{C}$, corresponds roughly to the observed variation.

Other measurements, not shown here, indicate that an important improvement in daily fluctuations of the apparent mass position can be obtained by shielding the system from external light. It seems that slight illumination differences during the day have an influence on the measured spot locations, which may explain especially the observed θ_z fluctuations.

Conclusions

Position and orientation of the mode cleaner masses can be measured with an optical scheme using the Annecy camera system. One camera with lens is sufficient for measuring $x, y, z, \theta_x, \theta_y, \theta_z$. Long- and short term precisions have been measured for the fine scheme; the results are summarized in Tab. 2.

	Fast fluctuations (rms values)				Slow drifts			
	needed		meas.	th. limit	needed		meas.	
	MC 30	MC 144				MC 30		MC 144
x	10	10	0.5 65	0.2 26	2000	2000	20	μm $\text{nm}/\sqrt{\text{Hz}}$
y	"	"	0.5 65	0.15 20	"	"	10	"
z	1	1	0.5 65	0.2 26	---	---	15	"
θ_x	9	7 (3)	1 130	0.08 10	45	35	15	μrad $\text{nrad}/\sqrt{\text{Hz}}$
θ_y	9	"	0.2 26	0.07 9	45	30	15	"
θ_z	10 000	"	20 2600	15 2000	---	"	100	"

Tab. 2: Results of the measurements, compared with the specifications (see Appendix 1) and with the theoretical limit, as imposed by the intrinsic camera noise. In parentheses, the specification valid for the case that the entrance bench is to be controlled locally even during VIRGO operation.

The orientation of the entrance bench determines the direction of the laser beam entering the interferometer. Therefore, during VIRGO operation, a reference signal for the beam alignment (θ_y and θ_z) should come from the VIRGO automatic alignment system, unless the specifications for the beam angle are not very critical. One should not rely only on the local mass control to stabilize the beam, also because of the danger of reintroduction of

seismic noise due to the ground-coupled reference system. Moreover, it does not seem very reasonable to align the whole interferometer on the output beam of the entrance bench.

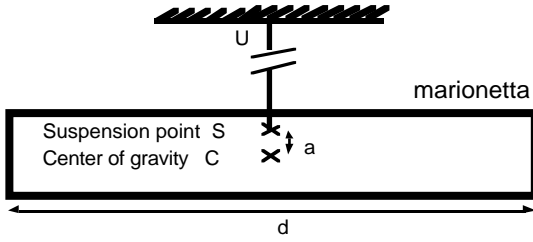


Fig. 4: The marionetta as a non-ideal pendulum.

In this case, i.e. if there is a global reference signal for the entrance bench orientation during VIRGO operation, the fine scheme fulfills the specifications. For θ_z , some improvement may be needed; this may e.g. come from limiting the unity gain frequency of the feedback: A factor of 7 can be gained in rms noise by limiting the feedback bandwidth to 1 Hz. If in practice

the θ_z control turns out to be too noisy, and the passive seismic isolation is not sufficient, then another possibility is to use the x damping to kill the θ_z resonance, since any pure rotation about the marionetta suspension point (Fig. 4) will quickly couple to a pendular motion around the upper wire suspension point, and therefore loose energy through the lateral damping in the x direction.

For a good precision of the local control system, a protection against air currents (box including the whole beam path) and ambient light is necessary.

From the long term behaviour it can be seen that, as was to be expected, memorizing the mass position works best for short times. Over periods of hours and days, thermal and other drifts reduce the accuracy with which one can come back to a predefined mass position.

Actual status

At present, the positions of the mode cleaner prototype masses can be read at a rate of 30 Hz, and first successful tests of calming the mass pendular movements by feedback to the marionetta magnet-coil system have been undertaken.

Appendix 1

Precision needed for determining the positions of the MC masses

		RC	MC 144	FP	MC 30
shape		Δ	Δ	–	Δ
length L	m	0.3	144	3000	30
mirror radius R	m	0.5	181	3450	85
waist $2w_0$	mm	0.58	9.9	39.6	7.4
Rayleigh length $2L_R$	m	0.44	147	2300	81
beam angle 2ϕ	μrad	2400	140	34	183
finesse F		50000	1000	50	1000

Tab. 3: Parameters of the reference cavity, the VIRGO mode cleaner, the arm cavities and the Orsay mode cleaner prototype, as needed for the calculations.

Static deviations

The specifications for the static accuracy of the system are given by the fact that the prealignment (using the values stored from a previous aligned state) must be precise enough to see fringes, i.e. to come into the linear regime where the autoalignment system can do the rest. For the angular resolution one has to demand e.g. $\theta_x/\theta_y < \phi/2$. If the far (curved) mirror is displaced in the x/y direction, this corresponds to a rotation $\theta_x=x/r$ or $\theta_y=y/r$; a curvature radius $r = 181$ m gives then a maximum x/y displacement of 6 mm; so this constraint is not very stringent. For a good centering of the beam on the mirrors, let

us demand an x/y resolution of 2 mm for the two masses. A z displacement of one of the masses just changes the cavity length, so there is no constraint at all within the range that can be corrected by the coil/magnet systems. For θ_z , it is supposed that the entrance bench (= mass 1 of the mode cleaner, with both flat mirrors) will be turned in order to steer its output beam into the interferometer. Thus, for a coarse prealignment, one should ask that the beam after 3 km hits the Fabry-Perot end mirror ($\varnothing=350\text{mm}$), whence one gets $\theta_y, \theta_z < 100\text{mm}/3\text{km}$ (for mass 1 of MC144 only).

Residual movements

The task of the local control system with respect to the mass movements is to damp pendular movements. Obviously, no reduction of the seismic noise floor (below or above resonance) can be achieved, since the local control system itself is coupled to seismic noise. These tasks are only valid during prealignment, or when for test purposes the MC is to be operated without automatic alignment.

The accuracy needed for the damping is determined for three cases:

First, for the nonlinear alignment it is necessary to damp the pendular oscillations enough in order to have a stable beam. This gives the same constraints as for the static case. Moreover, the longitudinal changes should be small enough in order to see interference fringes between beams having completed a different number of roundtrips. Therefore one can allow a z amplitude of the order of a wavelength. Since x/y movements can couple to the z component, their specifications should be perhaps 10 times the z limits.

Second, for the first phase of the prototype tests, and maybe for short test periods of the VIRGO MC, the cavity may be operated without automatic alignment. In this case, the mass oscillation should not disturb the MC resonance; thus, it should be small compared to the beam opening angle/waist; $\theta_x/\theta_y < \varphi/10$ seems a good value. For the MC144, the same is valid for θ_z , since the beam entering the entrance bench laterally from the laser bench will be mode matched to the MC. For the MC30, the argument is that, since a θ_z oscillation causes a displacement of the entrance beam on the flat mirrors, one should by the same argument have $\theta_z < w_0/10s$, where $2s$ is the distance of the two flat mirror centers.

Third: Let us suppose, that the local control of the MC mass positions will be active even during the normal VIRGO operation. If the MC masses oscillate, then the outgoing beam will do so also. The task of the MC is to deliver a clean TEM_{00} beam, where TEM_{00} is defined with respect to the fundamental mode resonant in VIRGO. Static deviations of beam position/angle can be corrected by the (slow) VIRGO autoalignment system, maybe acting on the entrance bench itself, but pendular movements occur around 1 Hz, which may be too fast. The $\text{TEM}_{01/10}$ contribution introduced by an uncorrected beam deviation is, given as a fraction of the TEM_{00} power:

$$\begin{aligned} \text{Beam displacement } \delta: & \quad \frac{2}{\pi} \left(\frac{\delta}{w_0} \right)^2 \\ \text{Beam tilt } \Theta: & \quad \frac{2}{\pi} \left(\frac{\Theta}{\varphi} \right)^2 \end{aligned}$$

w_0 is the waist, $\varphi = \lambda/\pi w_0$ the opening angle of the beam at the output of the entrance bench. Let's put a fractional power of 10^{-3} as an upper limit in the quasi-static regime below the GW frequency range, because else the TEM_{00} loses too much power; moreover, the distortions generated inside the interferometer by optics imperfections etc. are of the same order. From this follows $\delta < 200 \mu\text{m}$; $\Theta < 3 \mu\text{rad}$. Thus a reasonable requirement should be to say that the masses should not swing more than δ laterally and Θ angularly. This is a very strong requirement.

Taking the strongest limits from all arguments gives the constraints in Tab. 4.

	residual oscillations		static deviations		
	MC30	MC144	MC30	MC144	
x	10	10	2000	2000	μm
y	"	"	"	"	"
z	1	1	---	---	"
θ_x	9	7 (3)	45	35	μrad
θ_y	9	"	45	30	"
θ_z	10 000	"	---	"	"

Tab. 4: Allowed MC mass displacements / misalignments. Values in parentheses are valid if MC local control is active during VIRGO operation.

Appendix 2

Observation of reference marks and laser beams with a single camera.

Influence of the auxiliary mirror

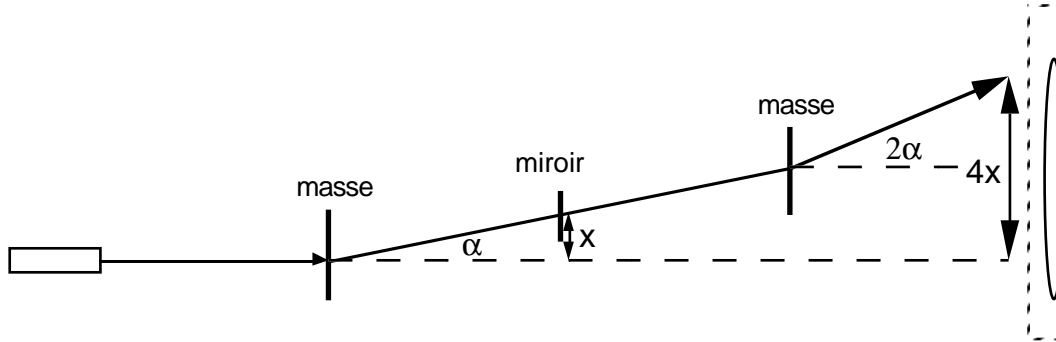


Fig. 7: Unfolded path of the "folded" laser beam, from laser over mass, auxiliary mirror, mass, to the camera lens.

The trajectory of the folded beam is shown in Fig. 7; the path of the direct beam is obtained by replacing the mirror by the camera. A mass rotation by $\alpha/2$ produces a displacement of the spot by $x=\alpha g$ for the one-way path (beam inclination α), and by $4x$ (inclination 2α) for the two-way path. A rotation $\alpha/2$ of the mass at distance g for the direct beam corresponds thus to a rotation α of a mass at $2g$ in the case of the folded beam. The lens collects all beams originating from a common point on the mass (= mass rotation) on one point on the CCD; the direct beam, without auxiliary mirror, has therefore zero sensitivity to rotations, which is not the case for the folded beam.

Influence of the lens on rotation measurements

The equivalent optical scheme for the folded beam is shown in Fig. 8. The lens is focused such as to create a sharp image of the mass: $1/b + 1/g = 1/f$, where f is the focal length of the lens. The image of the effective rotation point is at a distance B from the lens: $1/B + 1/G = 1/f$ ($G=2g$). The displacement X of the (non-perfectly focused) spot on the CCD screen, caused by a rotation $\alpha/2$ of the mass, is given by $X/(b-B) = 2\alpha G/B$, thus

$$X = 2\alpha G \frac{f}{2(g-f)} = 2\alpha G \frac{A}{2} .$$

The displacement of the spot (the sensibility to rotations) on the CCD is thus related to the displacement before the lens by a factor $A/2$, where $A = b/g < 1$ is the magnification of the CCD image with respect to the mass.

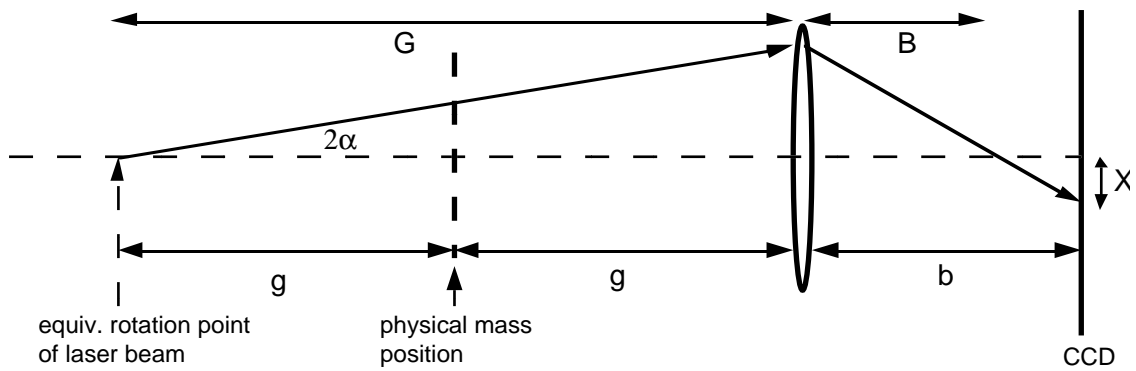


Fig. 8: Equivalent path of the folded laser beam.

Conclusion: Even with a lens one can observe at the same time the mass image and the laser spots giving the angular and z informations.

References

- [1] A. Bazan, R. Flaminio, P. Kramer, J.C. Lacotte, J. Lecoq, L. Massonnet, B. Mours, R. Morand, S. Tissot, D. Verkindt, M. Yvert, "A VME based imaging system for the VIRGO project"; *Astropart. Phys.* **2** (1994) 229.
- [2] J.C. Lacotte, B. Mours, S. Tissot, "Position resolution with the Annecy Beam Imaging System", VIRGO note PJT92032 (1992).
- [3] M.-C. Bollinger, "Notes sur la manip. sur la caméra pour le groupe VIRGO du L.A.L.", internal note Orsay (28.07.1994).
- [4] A. Bocchini, V. Ragozzino, "Note sul sistema di controllo locale delle masse sospese del mode cleaner", internal note Orsay (22.02.1995).

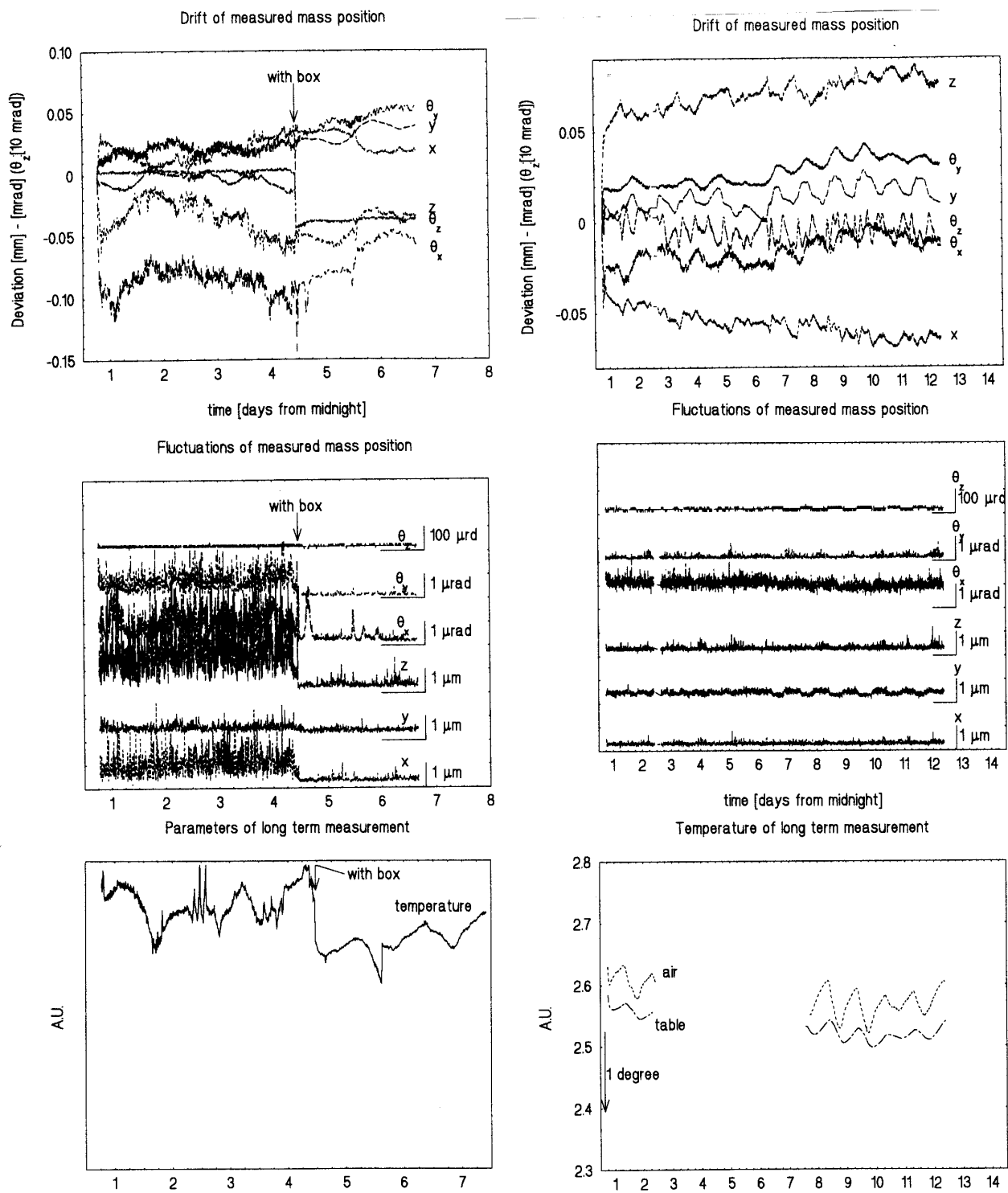


Fig. 5 (left): Measurement of the position of a fixed mirror in the table top experiment, using the fine measurement scheme. At the marked time, the experiment was covered with a Plexiglas box. **Fig. 6** (right): Measurement with Plexiglas box. **a)** apparent mass position. **b)** short term fluctuations **c)** air (and table) temperature near the mirror.